Adult-onset deficiency of acyl CoA:monoacylglycerol acyltransferase 2 protects mice from diet-induced obesity and glucose intolerance[S]

Taylor Banh,[1] David W. Nelson,[1] Yu Gao, Ting-Ni Huang, Mei-I Yen, and Chi-Liang E. Yen[2]

Department of Nutritional Sciences, University of Wisconsin-Madison, WI 53706

Abstract **Acyl-CoA:monoacylglycerol acyltransferase (MGAT) 2 catalyzes triacylglycerol (TAG) synthesis, required in intestinal fat absorption. We previously demonstrated that mice without a functional MGAT2-coding gene (*Mogat2*$^{-/-}$) exhibit increased energy expenditure and resistance to obesity induced by excess calories. One critical question raised is whether lacking MGAT2 during early development is required for the metabolic phenotypes in adult mice. In this study, we found that *Mogat2*$^{-/-}$ pups grew slower than wild-type littermates during the suckling period. To determine whether inactivating MGAT2 in adult mice is sufficient to confer resistance to diet-induced obesity, we generated mice with an inducible *Mogat2*-inactivating mutation. Mice with adult-onset MGAT2 deficiency (*Mogat2*^{AKO}) exhibited a transient decrease in food intake like *Mogat2*$^{-/-}$ mice when fed a high-fat diet and a moderate increase in energy expenditure after acclimatization. They gained less weight than littermate controls, but the difference was smaller than that between wild-type and *Mogat2*$^{-/-}$ mice. The moderate reduction in weight gain was associated with reduced hepatic TAG and improved glucose tolerance. Similar protective effects were also observed in mice that had gained weight on a high-fat diet before inactivating MGAT2. These findings suggest that adult-onset MGAT2 deficiency mitigates metabolic disorders induced by high-fat feeding and that MGAT2 modulates early postnatal nutrition and may program metabolism later in life.**—Banh, T., D. W. Nelson, Y. Gao, T-N. Huang, M-I. Yen, and C-L. E. Yen. **Adult-onset deficiency of acyl CoA:monoacylglycerol acyltransferase 2 protects mice from diet-induced obesity and glucose intolerance. *J. Lipid Res.* 2015.** 56: **379–389.**

Supplementary key words triacylglycerol • dietary fat • fat absorption • energy expenditure • metabolic programming • monoacylglycerol acyltransferase 2 • coenzyme A

Triacylglycerol (TAG) synthesis is crucial for many physiological processes involving storage or delivery of fatty acids and metabolic energy. TAG synthesis in most cells starts with acylation of glycerol-3-phosphate, followed by two additional acylation steps, whereas in some cells it uses monoacylglycerol (MAG) as the initial acyl acceptor. Acyl-CoA:monoacylglycerol acyltransferase (MGAT) catalyzes the latter pathway and generates diacylglycerol for the final acylation step (1). As MAG is mostly a degradation product of TAG, the MGAT pathway is thought to be important for recycling of TAG. Indeed, the best-characterized MGAT function is in the absorption of dietary fat. During the process, dietary TAG is hydrolyzed in the intestinal lumen to MAG and fatty acids. After uptake, the hydrolysis products are resynthesized to TAG in enterocytes for the assembly of chylomicron, which in turn delivers dietary lipids to peripheral tissues (2).

Among three identified genes encoding MGAT enzymes, *Mogat2* is highly expressed in the intestine of both rodents and humans (3–6). Supporting the role of MGAT2 as an intestinal MGAT mediating fat absorption, constitutive global inactivation of the enzyme, through germ-line transmission of a null mutation in *Mogat2*, greatly reduces intestinal MGAT activity and delays fat absorption (7). Interestingly, these *Mogat2*$^{-/-}$ mice absorb a normal quantity of fat but are protected from obesity and other metabolic disorders induced by high-fat feeding. The underlying physiological mechanisms involve a transient decrease in food intake and a persistent increase in energy expenditure (7, 8). Unexpectedly, the increase in energy expenditure does not require high-fat feeding, and MGAT2 deficiency also protects Agouti mice from excess weight gain (9). Findings from both gain- and loss-of-function mouse models indicate that MGAT2 in the intestine is a major contributor but incompletely accounts for the

This work was supported by grants from the National Institutes of Health (DK088210) and U.S. Department of Agriculture (WIS01442). T.B. was a recipient of a University of Wisconsin-Madison Undergraduate Research and Mentoring Fellowship as well as a Cargill-Benevenga Research Stipend for undergraduates.

Manuscript received 1 October 2014 and in revised form 2 December 2014.

Published, JLR Papers in Press, December 22, 2014
DOI 10.1194/jlr.M055228

Abbreviations: AUC, area under the curve; dpc, days postcoitus; MAG, monoacylglycerol; MGAT, monoacylglycerol acyltransferase; TAG, triacylglycerol.

[1] T. Banh and D. W. Nelson contributed equally to this work.

[2] To whom correspondence should be addressed.
e-mail: yen@nutrisci.wisc.edu

[S] The online version of this article (available at http://www.jlr.org) contains supplementary data in the form of one figure.

differences in body weight (8, 10), suggesting complex mechanisms underlying the role of MGAT2 in the regulation of systemic energy balance.

MGAT2 in mice is expressed in embryos as early as 7 days postcoitus (dpc) and in the liver and intestine during the perinatal period [NCBI UniGeneID:307396, Gene Expression Omnibus GDS3764, and (11, 12)], suggesting a potential role of MGAT2 during early development. Several lines of evidence in both human and rodent studies support the concept that nutritional status during early development, including embryonic and fetal as well as early postnatal periods, programs metabolism and propensity to gain weight later in life (13–19). For example, in a historical cohort study, exposure to the Dutch famine of 1944–1945 during the first half of pregnancy is associated with increased obesity rates in early adulthood, while exposure during the last trimester and the first months of life is associated with reduced obesity rates (20). In mice, early postnatal undernutrition limits adiposity induced by high-fat diet in adulthood (21). Thus, we question whether MGAT2 determines metabolic efficiency during early development and, more importantly, whether lacking MGAT2 during those critical periods is required for the protective effects against metabolic disorders seen in adult *Mogat2*$^{-/-}$ mice.

In this study, to determine whether MGAT2 plays a role in overall energy balance during the intrauterine and the suckling period, we examined body weights of fetuses at late gestation and of pups before weaning. In addition, to determine whether adult-onset MGAT2 deficiency is sufficient to modulate the responses to high-fat feeding, we developed inducible knockout mice in which MGAT2 could be ablated at specific developmental stages and examined their metabolic phenotypes in response to high-fat feeding.

MATERIALS AND METHODS

Mice

Germ-line MGAT2 knockout (*Mogat2*$^{-/-}$) mice with constitutive and global MGAT2 deficiency were produced as described (7). To enable inactivation of *Mogat2* in adult mice, a line of inducible MGAT2 knockout mice was generated using the Cre-loxP system with a ubiquitously expressed Cre recombinase that remains inactive until induction by tamoxifen treatment (22). *Mogat2*$^{f/f}$ mice carrying both copies of "floxed" *Mogat2* alleles with exon 2 flanked by Cre-recombinase target sites (loxP) (8) were crossed with a line of transgenic mice ubiquitously expressing a tamoxifen-inducible Cre recombinase [B6;Cg-Tg(UBC-cre/ERT2)1Ejb/J (23)]. Under the control of the ubiquitin C promoter, the inducible Cre recombinase is a fusion protein between Cre and a mutant form of the estrogen receptor, sequestering the enzyme in the endoplasmic reticulum. Cre activity is inducible by tamoxifen but not estrogen (23), which in turn mediates the precise excision of exon 2 of the *Mogat2* gene flanked by two *loxP* sites, switching off the functional gene. Through cross-breeding, inducible mutant (*Mogat2*^{im}) mice carrying "floxed" *Mogat2* alleles and one copy of the inducible *Cre* recombinase and their *Mogat2*$^{f/f}$ littermate controls were produced. Upon treatment with the estrogen analog tamoxifen, Cre translocates to the nucleus and excises exon 2 of the *Mogat2* gene in *Mogat2*^{im} mice, resulting in inactivation of MGAT2 (*Mogat2*^{AKO} mice).

Mice were housed on a 12 h light/dark cycle. Weighing of mice and changes of diets and cages were performed between 3 PM and 6 PM. All animal procedures were approved by the University of Wisconsin–Madison Animal Care and Use Committee and were conducted in conformity with the Public Health Service Policy on Humane Care and Use of Laboratory Animals.

Tamoxifen treatment to inactivate MGAT2

To inactivate MGAT2, adult *Mogat2*^{im} and *Mogat2*$^{f/f}$ control mice were intragastrically administered a daily dose of tamoxifen (MP Biomedicals; 200 mg/kg body weight/day; 20 mg/ml in corn oil) for 5 days either at 4 months of age (prior to high-fat feeding) or at 5 months of age (after 7 weeks of high-fat feeding). Because tamoxifen treatment causes a transient decrease in body weight (data not shown), we allowed mice to recover for 1 month before performing energy balance experiments. Tamoxifen-induced weight loss was also observed in diet-induced obese mice.

Genotyping

Genotypes of mice were determined by PCR. To determine the presence of the Cre-recombinase transgene, the following four primers were used: Cre forward, 5′-CCCGGCAAAACAGG-TAGTTA-3′; Cre reverse, 5′-TGCCAGGATCAGGGTTAAG-3′; Positive control forward, 5′-CCTTTAGCCTGGTCTAGGCA-GAG-3′; and Positive control reverse, 5′-CAGCAAAGCCCCC-TCCTGAATCTCTC-3′. This reaction produces a 194 bp amplicon and a 381 bp amplicon from the transgene and the internal control gene, respectively. To determine the presence of the wild-type or floxed *Mogat2* allele, the following two primers were used: *Mogat2* forward, 5′-GTATGCCACCTGGTGGTAC-3′; and *Mogat2* reverse, 5′-GCAGTCCTATACCAGTACAG-3′. This reaction produces a 478 bp amplicon and a 512 bp amplicon from the wild-type allele and the allele with the addition of a 34 bp loxP site, respectively. To confirm Cre-recombinase-mediated deletion of *Mogat2* following tamoxifen treatment we regenotyped mice using the same *Mogat2* primers plus an additional primer, Target forward, 5′-GAACTTCGTCGAGATAACTTCGT-3′, specific for a region upstream of the floxed allele. This reaction produces 512 and 1,089 bp amplicons prior to excision, and a 191 bp amplicon after excision.

Diets

Mice were fed a complete, fixed-formula chow (#8604; Teklad, Madison, WI). A series of semipurified (defined) diets containing 10, 45, or 60% calories from fat (D12450B, D12451, and D12492; Research Diets, New Brunswick, NJ) were used to examine the effect of dietary fat on food intake and energy expenditure, as indicated. These defined diets contained 20% calories from protein (casein) and fixed amounts of micronutrients and fiber per calorie, but they varied in metabolizable energy (3.8, 4.7, or 5.2 kcal/g), corresponding to the fat content.

Real-time quantitative PCR analysis

The levels of *Mogat2* mRNA in tissues collected from fetuses of embryonic day 19 or mice fed the 60 kcal% fat diet for 10 weeks were assessed as previously described (8). Cyclophilin B (*Cypb*) expression was used as an internal control. The primer sequences of the *Cypb* gene were 5′TGCCGGAGTCGACAATGAT-3′ (forward) and 5′-TGGAAGAGCACCAAGACAGACA-3′ (reverse). The primers to

detect *Mogat2* mRNAs were located on exon 1 and exon 2, respectively; the forward primer sequence was 5′- TGGGAGCG-CAGGTTACAGA-3′, and the reserve primer sequence was 5′- CAGGTGGCATACAGGACAGA-3′. The $2^{-\Delta\Delta Ct}$ method was used to calculate the fold change in gene expression (24).

In vitro MGAT assays

MGAT activity assays were performed with total tissue homogenates as previously described (10). Reactions were started by adding total tissue homogenates to the assay mixture and were stopped by adding chloroform-methanol (2:1, v/v). The lipids were extracted, dried, and separated by TLC on silica gel G-60 TLC plates with hexane-diethyl ether-acetic acid (80:20:1, v/v/v). Lipid bands were visualized with iodine vapor, and products were identified by comparison with the migration of lipid standards. The incorporation of radioactive substrates into lipid products was also visualized by an imaging scanner (Typhoon FLA 7000; GE Healthcare Life Sciences, Piscataway, NJ) followed by band scraping and counting in a scintillation counter analyzer (Packard Tri-Carb 2200 CA Liquid Scintillation Counter Analyzer; PerkinElmer, Santa Clara, CA).

Metabolic phenotyping studies

To assess phenotypes related to acute energy balance, mice were housed in a metabolic phenotyping system with housing and wood chip bedding similar to the home cage environment (LabMaster modular animal monitoring system; TSE, Chesterfield, MO). Adult male mice were acclimated to individual housing and metabolic cages for 1 week before experiments and were fed indicated diets sequentially for 3 days each. Data collection and analysis were performed as previously reported (9, 10).

Body weight response to chow or high-fat feeding

We monitored weight gains daily before weaning and weekly afterward to assess long-term energy balance. To examine long-term body weight responses to low-fat chow and high-fat diet, male mice were fed a regular mixed meal chow at weaning (3 weeks) and then switched to a 60% diet at 4 months of age and for an additional 10 weeks. To investigate the effect of MGAT2 inactivation in diet-induced obese mice, male mice were switched to the 60 kcal% fat diet at 2–3 months of age, prior to inactivation of MGAT2.

Biochemical assays

Plasma lipids were assayed using enzymatic kits (Infinity™ Triglycerides Lipid Stable Reagent, Thermo Fisher; Cholesterol E, Non Esterified Fatty Acid assay, Wako Diagnostics). Hepatic and fecal lipids were extracted in chloroform-methanol (2:1, v/v) following homogenization in PBS. Blood samples were collected from the orbital plexus, and plasma was separated by centrifugation. Hepatic TAG and glycogen were measured as described previously (8). Protein concentration was measured by Pierce BCA Protein Assay Kit (Thermo, Rockford, IL). To examine glucose metabolism following high-fat feeding, mice were fed 60 kcal% fat diet for ∼8 weeks, then a glucose tolerance test was performed. Briefly, male mice were fasted for 6 h beginning at 7 AM and then injected with glucose (1 g/kg bodyweight, ip, 10% glucose in PBS). Blood glucose was measured immediately before and at defined intervals after glucose injection using a handheld glucose monitor (OneTouch Ultra; LifeScan Inc., Milpitas, CA). Plasma insulin was measured by ELISA (Crystal Chem Inc., Downers Grove, IL).

Statistical analyses

All data are presented as mean ± SEM. $P < 0.05$ was considered statistically significant. Each experiment was performed with independent samples at least twice to confirm reproducibility of the results. For comparisons between two groups, Student's *t*-tests were used. Differences measured over time were compared using repeated-measures two-way ANOVA to determine main effects of, and interactions between, time and genotype. To identify group differences, Bonferroni's posttests were performed. Analyses were conducted using GraphPad Prism statistical analysis software (version 5.01; GraphPad Software, La Jolla, CA).

RESULTS

Mouse pups with constitutive *Mogat2* inactivation gain less weight during the suckling period

To explore a potential role of MGAT2 during early development, we first assessed if its coding gene *Mogat2* is expressed prenatally in fetal tissues collected on embryonic day 19 (dpc) using quantitative PCR. We found high levels of MGAT2 mRNA in intestine, similar to in adult mice. Relatively moderate levels of MGAT2 were also found in yolk sac, liver, and kidney, but not in placenta (**Fig. 1A**). We next compared body weights of fetuses at a late stage of gestation (19 dpc) from intercrosses of heterozygous mice ($Mogat2^{+/-}$), bearing a constitutively null *Mogat2* allele. We found no difference in intrauterine growth between wild-type, $Mogat2^{+/-}$, and $Mogat2^{-/-}$ fetuses (Fig. 1B), suggesting that MGAT2 does not play an indispensable role in the regulation of energy balance during the prenatal period. In contrast, after birth, pups with the germ-line null mutation ($Mogat2^{-/-}$) gained less weight than wild-type littermates throughout the suckling period, when pups nursed on milk rich in fat [∼20% by weight (25)] (Fig. 1C). At weaning, their average weight was ∼80% that of controls. Consistent with previous reports (7, 9), after weaning onto a standard low-fat chow, these mice exhibited compensatory growth and were able to reach a body weight similar to wild-type littermates by 3 months of age (Fig. 1D). When their feed was switched to a diet containing 60% calories from fat, wild-type mice gained significantly more weight than did $Mogat2^{-/-}$ littermates (Fig. 1E). During 10 weeks of high-fat feeding, wild-type mice gained on average 20.2 ± 1.6 g while $Mogat2^{-/-}$ mice gained only 4.7 ± 0.3 g (Fig. 1E).

Generation of mice with tamoxifen-inducible *Mogat2* inactivation

To determine whether MGAT2 deficiency during early development is required for the obesity-resistant phenotype seen in $Mogat2^{-/-}$ mice, we developed a mouse model in which *Mogat2* can be inactivated in adulthood. Mice carrying a tamoxifen-inducible ubiquitin-Cre recombinase were crossed with mice carrying two *loxP* sites flanking exon 2 of the *Mogat2* gene (8). The offspring were intercrossed to generate mice carrying homozygous "floxed" *Mogat2* alleles ($Mogat2^{f/f}$), and half of them were also hemizygous, carrying a copy of the transgene expressing the inducible Cre recombinase ($Mogat2^{f/f}$, $UBC\text{-}Cre^{+}$). Before induction, these inducible mutants are designated $Mogat2^{im}$ mice.

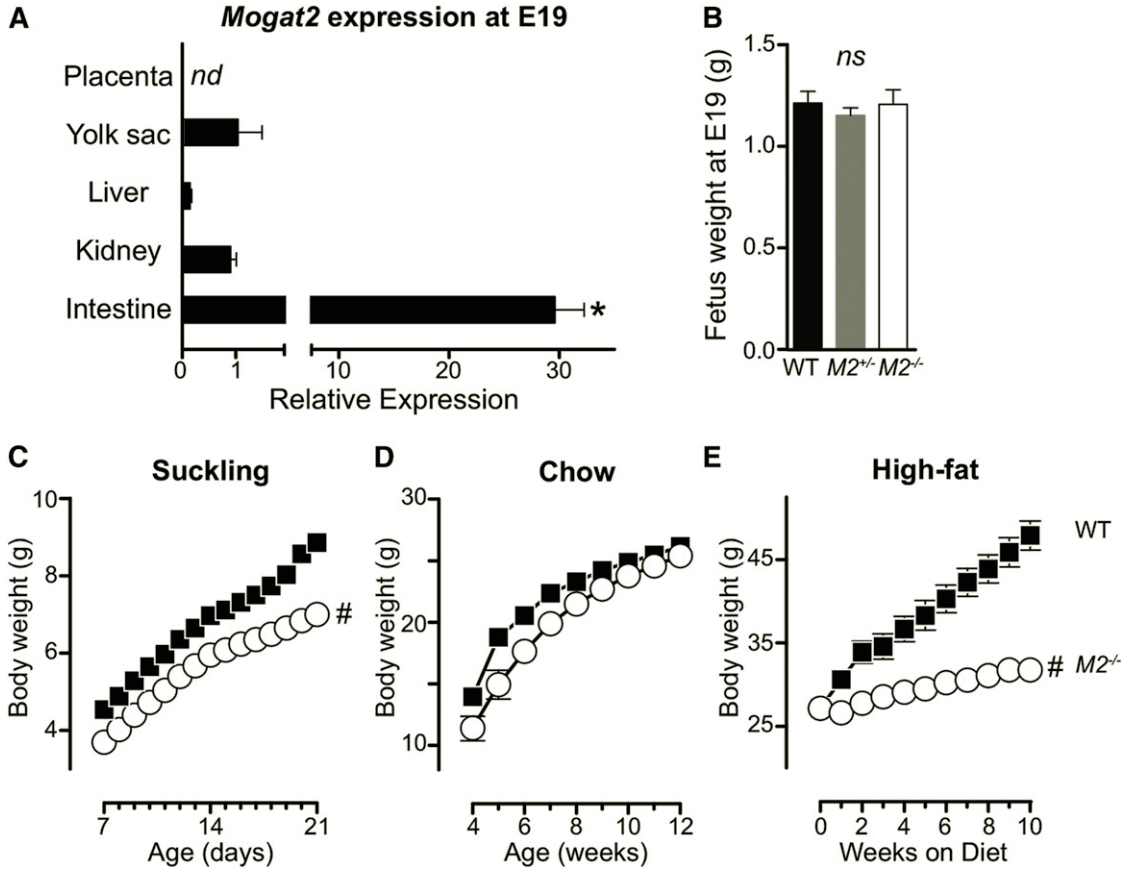

Fig. 1. MGAT2 expression and body mass of fetuses as well as growth curves of mice. A: *Mogat2* expression in tissues of wild-type mouse fetus collected on embryonic day 19 (E19). * $P < 0.05$ versus all other tissues by Dunnett's test. *nd*, not detected. B: Body weight of wild-type (WT), *Mogat2*$^{+/-}$ (*M2*$^{+/-}$), and *Mogat2*$^{-/-}$ (*M2*$^{-/-}$) fetuses on day E19. $n = 4$–12 per group. Bars represent mean ± SEM. *ns*, no significant difference. C: Daily body weight of pups during the suckling period. Weekly body weight of mice consuming chow (D) or 3-month-old mice consuming 60 kcal% fat diet (E). $n = 12$–27 mice per group. Error bars represent SEM and are not shown when smaller than the symbols. # $P < 0.05$ versus littermate controls by repeated-measures ANOVA.

To inactivate *Mogat2* in adulthood, we treated *Mogat2*^{im} mice with tamoxifen at 12 weeks of age. Tamoxifen treatment resulted in deletion of *Mogat2* exon 2 in *Mogat2*^{im} mice, but not in their *Mogat2*$^{f/f}$ littermate controls, as confirmed by PCR using genomic DNA (data not shown). These mice with *Mogat2* inactivated in adulthood by tamoxifen-mediated Cre-recombinase induction were designated "adult-onset knockout" (*Mogat2*^{AKO}). To assess the specificity as well as efficiency of *Mogat2* ablation, we measured *Mogat2* mRNA expression level in these mice. Before tamoxifen treatment, both *Mogat2*$^{f/f}$ and *Mogat2*^{im} mice expressed levels of *Mogat2* mRNA in small intestine similar to that found in wild-type mice (**Fig. 2A**). As reported previously (7, 8), *Mogat2*$^{-/-}$ mice had no detectable *Mogat2* mRNA (Fig. 2A). In contrast, following tamoxifen treatment, *Mogat2*$^{f/f}$ mice maintained their *Mogat2* mRNA levels while *Mogat2*^{AKO} mice showed very low levels of expression in the small intestine (Fig. 2A). Similar relative expression levels among genotypes were also found in the kidney and white adipose tissue (supplementary Fig. 1), confirming the efficiency of *Mogat2* deletion by the inducible Cre recombinase. Tissues examined were collected from mice after 10 weeks of high-fat feeding. The lasting MGAT2 deficiency indicates that the tamoxifen treatment was efficient in activating Cre recombinase and causing *Mogat2* ablation in the intestinal stem cells, which normally replace intestinal epithelia every 3–5 days (26).

Mogat2 mRNA levels correlated with MGAT activity in the small intestine. Before tamoxifen treatment, *Mogat2*$^{f/f}$ and *Mogat2*^{im} mice showed MGAT activity similar to that of wild-type mice (Fig. 2B). Ablation of MGAT2 expression in adulthood by tamoxifen treatment reduced intestinal MGAT activity in *Mogat2*^{AKO} mice to levels similar to those in constitutive germ-line *Mogat2*$^{-/-}$ mice (Fig. 2B). These results indicate that tamoxifen treatment effectively transforms adult inducible mutant *Mogat2*^{im} mice into adult-onset MGAT2-deficient *Mogat2*^{AKO} mice.

Before inactivation of MGAT2, inducible mutant mice exhibit normal energy balance and gain weight like controls

Before tamoxifen treatment, the inducible mutant *Mogat2*^{im} pups gained weight normally during the suckling period like their *Mogat2*$^{f/f}$ littermates (**Fig. 3A**). After weaning, when mice were fed a low-fat chow, these mice continued to grow at a similar rate as control mice did into

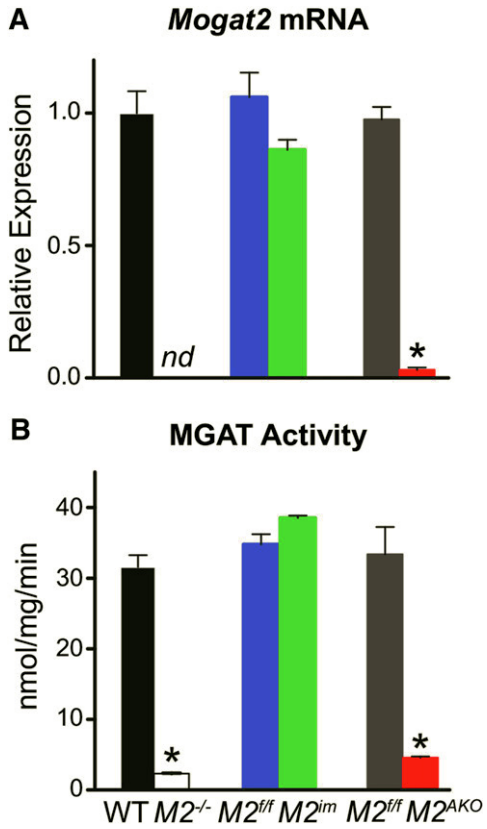

Fig. 2. Generation of the tamoxifen-inducible *Mogat2*-deficient mouse. Efficiency and specificity to tamoxifen-mediated deletion of *Mogat2* were confirmed by measuring *Mogat2* mRNA level (A) and MGAT activity (B) in the jejunum of wild-type (WT, black), $Mogat2^{-/-}$ ($M2^{-/-}$, white), $Mogat2^{f/f}$ ($M2^{f/f}$, blue), $Mogat2^{im}$ ($M2^{im}$, green), tamoxifen-treated $Mogat2^{f/f}$ ($M2^{f/f}$, gray), and tamoxifen-treated $Mogat2^{im}$ (adult-onset knockout, $M2^{AKO}$, red) mice. $n = 3$–14 mice per group. Bars represent mean ± SEM. *nd*, not detected. * $P < 0.05$ versus littermate controls by *t*-test.

adulthood (Fig. 3B). To further confirm that the inducible Cre recombinase does not affect energy metabolism prior to induction, we characterized acute energy balance of these mice in response to a regular low-fat chow diet and three semipurified diets containing 10, 45, or 60% of calories from fat sequentially by indirect calorimetry. Both food intake and energy expenditure, reflected by oxygen consumption (VO_2), were similar between $Mogat2^{f/f}$ and $Mogat2^{im}$ mice (Fig. 3C, D), resulting in parallel body weight changes during each of the diet treatments (Fig. 3E). Both groups of mice gained 2.5 g of body weight after being fed the semipurified diets for 9 days. Consistently, both $Mogat2^{f/f}$ and $Mogat2^{im}$ mice gained on average 22.3 g of excess body weight after 10 weeks of high-fat feeding (Fig. 3F). These data indicate that expressing UBC-Cre recombinase has no effect on energy metabolism before tamoxifen-induced activation.

Adult-onset MGAT2 deficiency modulates energy balance and protects mice against diet-induced weight gain

We next determined the effect of MGAT2 inactivation in adulthood on acute energy balance in response to the same four diets. $Mogat2^{AKO}$ mice were produced by treating 3-month-old chow-fed $Mogat2^{im}$ mice with tamoxifen to induce *Mogat2* deletion. As controls, their $Mogat2^{f/f}$ littermates were also subjected to the same treatment. Indirect calorimetry was performed 1 month after treatment to allow for recovery of stable body weight. When fed chow or the semipurified diet containing 10 kcal% fat, $Mogat2^{AKO}$ mice exhibited levels of food intake, respiratory exchange ratio (RER), and energy expenditure similar to those of $Mogat2^{f/f}$ controls (**Fig. 4A**–C). Though all levels trended higher in $Mogat2^{AKO}$ mice, the differences did not reach statistical significance. When first exposed to high-fat diets (45 kcal% and 60 kcal% fat for 3 days each), $Mogat2^{AKO}$ mice reduced food intake significantly as compared with $Mogat2^{f/f}$ controls (Fig. 4A). The difference disappeared after 1 week of high-fat feeding (Fig. 4A), similar to that reported in mice with constitutive global MGAT2 deficiency as well as those with intestine-specific deficiency (8, 9). Associated with decreases in food intake, $Mogat2^{AKO}$ mice exhibited a lower RER than $Mogat2^{f/f}$ controls when first exposed to high-fat feeding (Fig. 4B), suggesting an increase in fat oxidation and/or a decrease in fat accretion. $Mogat2^{AKO}$ mice did not exhibit significant elevations in energy expenditure until they were acclimated to high-fat feeding. They showed a significant 13% increase in 24 h energy expenditure compared with $Mogat2^{f/f}$ mice when food intake was similar between groups (Fig. 4A, C).

$Mogat2^{AKO}$ and $Mogat2^{f/f}$ mice did not differ in energy balance, as indicated by similar body weights when fed chow or the 10% fat diet (Fig. 4D). When fed the high-fat diets, $Mogat2^{AKO}$ mice maintained their body weight, while $Mogat2^{f/f}$ mice gained weight during the metabolic chamber studies (Fig. 4D). After acclimatization to high-fat feeding, $Mogat2^{AKO}$ mice absorbed similar amounts of dietary fat as $Mogat2^{f/f}$ mice did, as indicated by similar levels of fecal output and fecal fat (Fig. 4E).

The differences in body weights increased throughout the following 10 weeks of high-fat feeding (**Fig. 5A**). $Mogat2^{AKO}$ mice gained only 65% as much as $Mogat2^{f/f}$ controls (12 g vs. 19 g, respectively). The differences were largely due to differences in fat mass. White and brown adipose tissues were significantly smaller in $Mogat2^{AKO}$ mice compared with $Mogat2^{f/f}$ controls (both ~70% of controls; Fig. 5B). Lean mass, represented by calf and heart, was not different across genotypes (Fig. 5B).

Adult-onset MGAT2 deficiency protects mice from diet-induced hepatic steatosis and glucose intolerance

Constitutive MGAT2 deficiency protects $Mogat2^{-/-}$ mice from several metabolic disorders induced by high-fat feeding (7). Thus, we next examined whether inactivation of MGAT2 in adulthood was sufficient to protect $Mogat2^{AKO}$ mice from comorbidities associated with obesity. After 10 weeks of high-fat feeding, $Mogat2^{AKO}$ mice had similar levels of TAG and free fatty acids but a moderately lower level of total cholesterol in fasting plasma, compared with $Mogat2^{f/f}$ mice (**Fig. 6A**–C). Like wild-type mice, after long-term high-fat feeding, $Mogat2^{f/f}$ mice developed hepatic

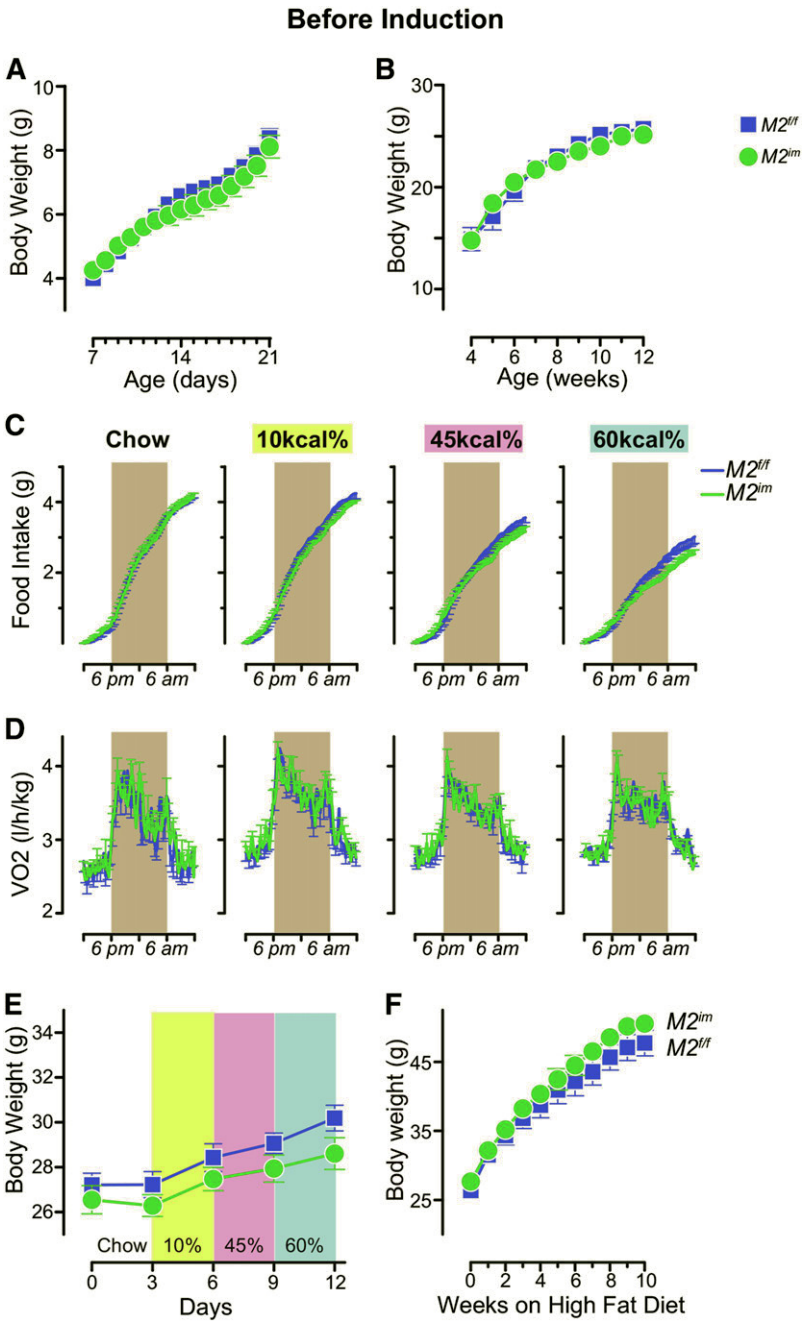

Fig. 3. No difference in energy balance before inactivation of MGAT2. Body weight of *Mogat2*$^{f/f}$ (*M2*$^{f/f}$, blue squares) and *Mogat2*^{im} (*M2*^{im}, green circles) mice during suckling (A) and chow feeding (B). n = 9–19 mice per group. C–E: Three-month-old mice sequentially fed chow or defined diets containing 10, 45, or 60% calories from fat for 3 days per diet. Cumulative food intake (C) and oxygen consumption rates (D) adjusted for baseline body weights of each mouse at the start of each diet treatment. Data from each mouse were pooled from the same time of the day of the same diet treatment. Graphs represent average days. Gray areas mark dark phase of the light cycle (6 PM to 6 AM). E: Body weight of mice during 12-day metabolic phenotyping experiment. n = 8 per group. F: Body weight of mice during 10 weeks of high-fat feeding. n = 9 or 13.

steatosis as indicated by increased liver mass and TAG content (Fig. 6D, E). Meanwhile, *Mogat2*^{AKO} mice were protected and had smaller livers and lower TAG content than *Mogat2*$^{f/f}$ controls. Hepatic glycogen was not different across genotypes (Fig. 6F). In parallel with accumulation of liver TAG, *Mogat2*$^{f/f}$ mice developed impaired glucose tolerance, while *Mogat2*^{AKO} mice were protected. After 8 weeks of high-fat feeding, *Mogat2*^{AKO} mice had lower fasting glucose than *Mogat2*$^{f/f}$ controls (191 mg/dl vs. 238 mg/dl) and a blunted increase in blood glucose following an intraperitoneal glucose challenge (AUC, 80% of controls; Fig. 6G). Further, *Mogat2*^{AKO} mice had lower plasma insulin concentrations right before as well as after glucose challenge (Fig. 6H), which was consistent with greater insulin sensitivity.

Inactivation of MGAT2 in obese mice reduces body weight and improves glucose tolerance

To examine the effects of inactivating MGAT2 in diet-induced obese mice, we fed 3-month-old adult *Mogat2*$^{f/f}$ and *Mogat2*^{im} mice a high-fat diet for 7 weeks. Both *Mogat2*$^{f/f}$ and inducible *Mogat2*^{im} mice gained weight before tamoxifen treatment (**Fig. 7A**). During the 5-day tamoxifen treatment, both groups of mice lost similar amounts of body weight. Whereas *Mogat2*$^{f/f}$ mice resumed high-fat diet-induced weight gain within 2 weeks of tamoxifen treatment, *Mogat2*^{AKO} mice continued to lose weight for an additional week. *Mogat2*^{AKO} mice weighed significantly less than *Mogat2*$^{f/f}$ littermates, and the difference increased throughout the remainder of the study (Fig. 7A). The reduction in

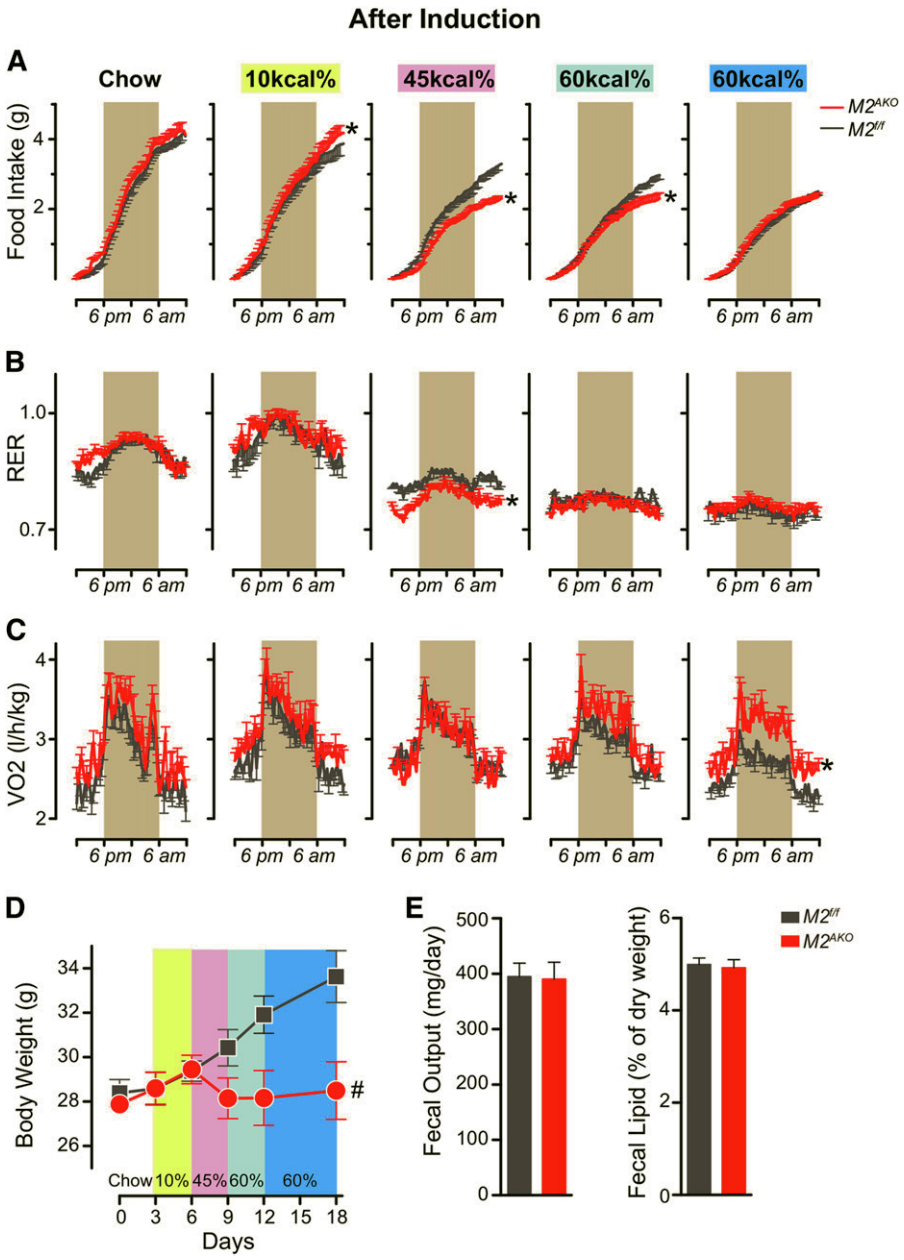

Fig. 4. Inactivation of MGAT2 in adulthood alters energy balance upon high-fat feeding. A–C: Four-month-old tamoxifen-treated *Mogat2*$^{f/f}$ (*M2*$^{f/f}$, gray) and tamoxifen-treated adult-onset MGAT2-deficient (*M2*^{AKO}, red) mice sequentially fed chow or defined diets containing 10, 45, or 60% calories from fat for 3 days per diet. Mice were fed the 60 kcal% diet for an additional 6 days. Cumulative food intake (A), RER (B), and oxygen consumption rates (C) adjusted for baseline body weights of each mouse at the start of each diet treatment. Data from each mouse were pooled from the same time of the day of the same diet treatment. Graphs represent average days. Gray areas mark dark phase of the light cycle (6 PM to 6 AM). D: Body weight of mice during 18-day metabolic phenotyping experiment. $n = 7$ or 6. E: Fecal output and lipid content of mice after acclimatization to high-fat feeding. Error bars represent SEM. Error bars not shown are smaller than the symbols. * $P < 0.05$ versus littermate controls by *t*-test [total cumulative mass for food intake, 24 h average for RER, and area under the curve (AUC) for VO_2]. # $P < 0.05$ versus littermate controls by repeated-measures ANOVA.

weight gain was associated with significantly reduced liver and white adipose mass (Fig. 7B). Lean mass (as indicated by calf and heart) was not different between genotypes (Fig. 7B).

After 6 weeks of high-fat feeding, glucose metabolism was impaired in both *Mogat2*^{im} and *Mogat2*$^{f/f}$ mice as illustrated by high fasting glucose (219 ± 9 mg/dl vs. 218 ± 12 mg/dl) and insulin levels (1.9 ± 0.4 ng/ml vs. 2.5 ± 0.5 ng/ml), respectively. Response to an oral glucose challenge was similar in both groups of mice (Fig. 7C, left panel). When the same test was administered 3 weeks after *Mogat2* inactivation, both levels of fasting blood glucose and insulin were lower in *Mogat2*^{AKO} than those of controls (Fig. 7C, middle panel; data not shown). In addition, the blood

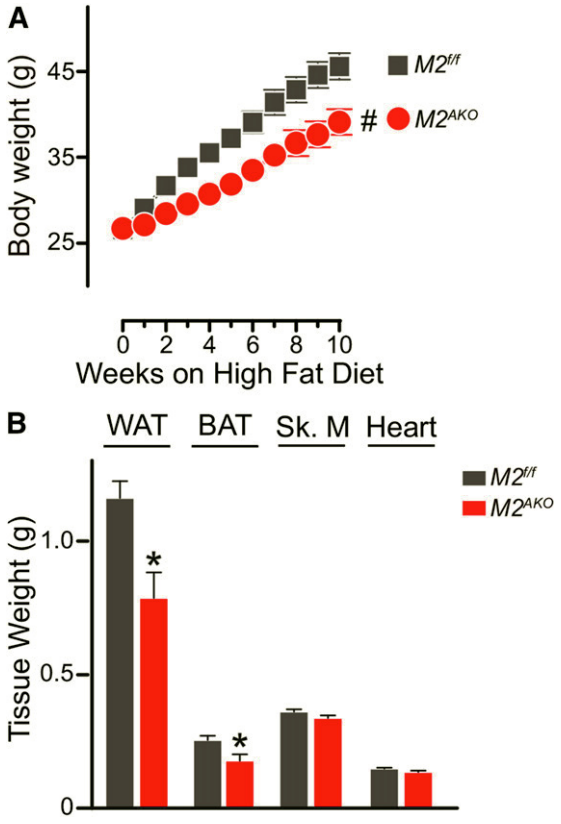

Fig. 5. Inactivation of MGAT2 partially protects weight gain induced by high-fat feeding. A: Body weight of post-tamoxifen-treated mice during 10 weeks of high-fat feeding. $n = 16$ or 18. $^{\#}$ $P < 0.05$ versus littermate controls by repeated-measures ANOVA. B: Tissue mass of mice following 10 weeks of high-fat feeding. $n = 11$ or 12. * $P < 0.05$ versus littermate controls.

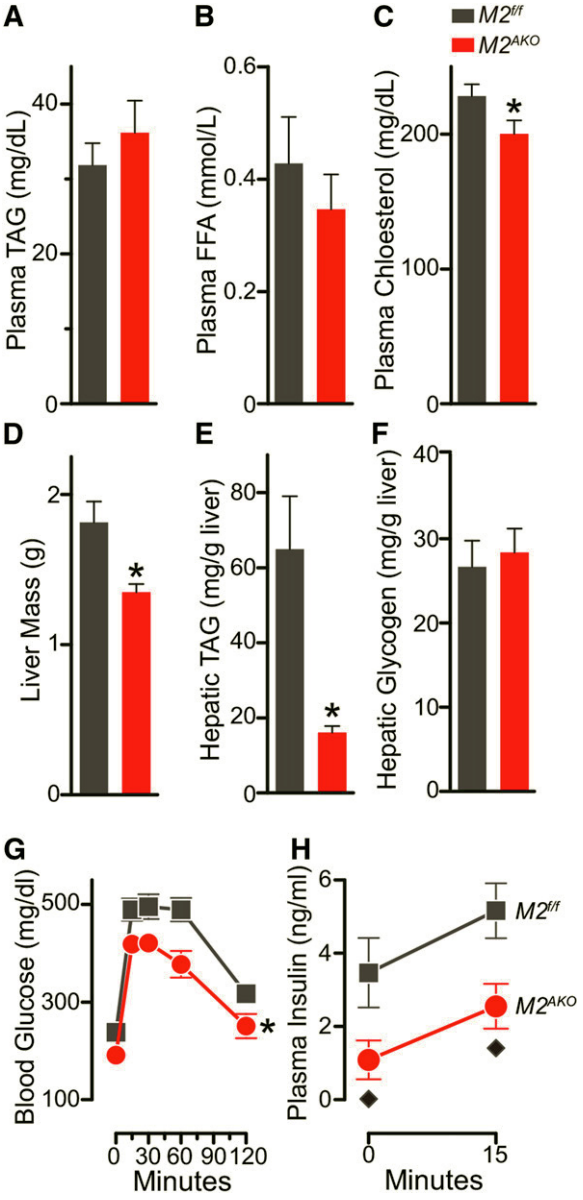

Fig. 6. Inactivation of MGAT2 protects against hepatic steatosis and impaired glucose metabolism. Plasma TAG (A), plasma free fatty acids (B), plasma cholesterol (C), liver mass (D), hepatic TAG (E), and hepatic glycogen (F) in tamoxifen-treated *Mogat2*$^{f/f}$ (*M2*$^{f/f}$, black) and adult-onset MGAT2-deficient (*M2*^{AKO}, red) mice fed 60 kcal% fat diet for 10 weeks. $n = 6$ or 9. Bars represent mean ± SEM. Blood glucose (G) and plasma insulin (H) in 8-week high-fat fed mice before and at indicated times after an intraperitoneal injection of glucose (1 mg/g body weight, 10% glucose in PBS). $n = 9$ or 11 per group. * $P < 0.05$ versus littermate controls by *t*-test (mean for plasma cholesterol, liver mass and TAG, and AUC for blood glucose). ◆ $P < 0.05$ versus time-matched littermate controls by *t*-test.

glucose levels in *Mogat2*^{AKO} mice did not rise as high as in tamoxifen-treated *Mogat2*$^{f/f}$ controls (Fig. 7C, middle panel). After adjusting for blood glucose levels right before the challenge, the net AUC in *Mogat2*^{AKO} mice was 66% of that in controls (Fig. 7C, middle panel, inset). The differences were even more pronounced after prolonged high-fat feeding (10 weeks after *Mogat2* inactivation). Blood glucose levels rose to a lower level and declined faster in *Mogat2*^{AKO} mice than in *Mogat2*$^{f/f}$ controls (Fig. 7C, right panel).

DISCUSSION

We have previously reported that constitutive inactivation of MGAT2 through a null mutation in the germ line protects *Mogat2*$^{-/-}$ mice against obesity and associated metabolic disorders induced by high-fat feeding as well as by the Agouti mutation (7, 9). In this study, we showed that *Mogat2*$^{-/-}$ mice experience undernutrition during the early postnatal period, as suckling *Mogat2*$^{-/-}$ pups gained less weight than their wild-type littermates. To determine whether MGAT2 deficiency during early development is essential for the effects on energy balance, we generated mice with adult-onset MGAT2 deficiency. We found that MGAT2 inactivation during adulthood is sufficient to decrease metabolic efficiency and the propensity to gain weight upon high-fat feeding. Before inducing the deletion of MGAT2, *Mogat2*^{im} mice exhibited energy balance similar to wild-type mice during the suckling period as well as upon high-fat feeding. After the ablation of MGAT2 in adulthood, *Mogat2*^{AKO} mice exhibited a transient decrease in food intake when fed a high-fat diet and a persistent increase in energy expenditure after acclimatization to high-fat feeding. These findings indicate that inactivating

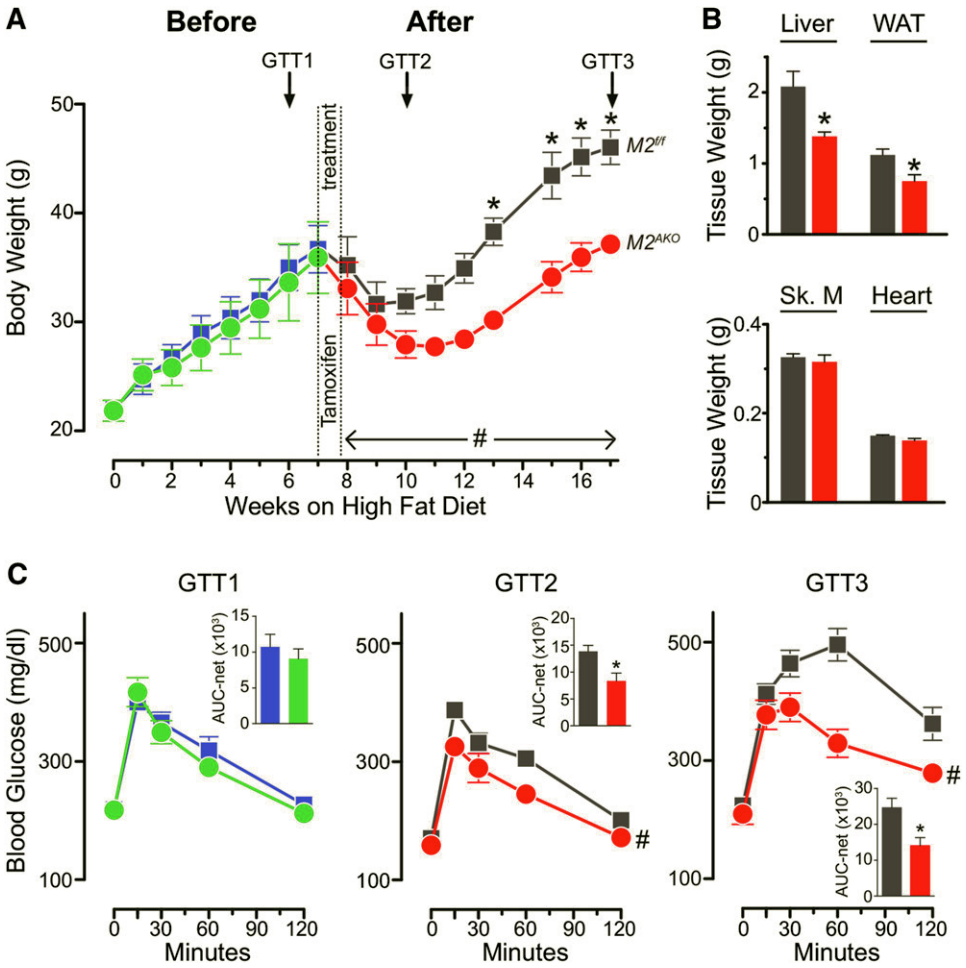

Fig. 7. Inactivation of MGAT2 in diet-induced obese mice attenuates further weight gain and improves glucose tolerance. A: Body weight of mice during high-fat feeding before and after inactivation of MGAT2. $n = 5$ mice per group. GTT1, GTT2, and GTT3 indicate time of glucose tolerance tests. # $P < 0.05$ by repeated-measures ANOVA after tamoxifen treatment, respectively. * $P < 0.05$ versus littermate controls by Bonferroni test. B: Tissue mass of mice following 10 weeks of post-tamoxifen treatment high-fat feeding. * $P < 0.05$ versus littermate controls. C: Blood glucose before and at indicated times after an intragastric challenge of glucose (200 μl of 10% glucose) in high-fat fed mice before (left panel), 3 weeks after (middle panel), and 10 weeks after (right panel) inactivation of MGAT2. Inset: net AUC. $n = 8$–10 mice per group. * $P < 0.05$ versus littermate controls by *t*-test. Color scheme for all panels: *Mogat2*$^{f/f}$ (*M2*$^{f/f}$, blue), *Mogat2*^{im} (*M2*^{im}, green), tamoxifen-treated *Mogat2*$^{f/f}$ (*M2*$^{f/f}$, gray), and tamoxifen-treated *Mogat2*^{im} (adult-onset knockout, *M2*^{AKO}, red) mice.

MGAT2 in adult mice is sufficient to confer resistance to obesity induced by diet. However, the protection against weight gain observed in *Mogat2*^{AKO} mice was to a lesser extent than in *Mogat2*$^{-/-}$ mice, raising the possibility that the early postnatal nutrition status may modulate energy balance phenotypes observed in *Mogat2*$^{-/-}$ mice later in life.

The expression of *Mogat2* in mice has been reported during early development in 7-day embryos [RIKEN full-length enriched library (27); GenBank accession number: AK049560.1]. Its expression in fetal intestine is relatively low 6 days before birth but reaches levels as high as those in adults during perinatal periods (12). In tissues from E19 fetuses, we found a high level of *Mogat2* expression in the intestine (Fig. 1A), consistent with a role of MGAT2 in mediating the absorption of milk fat soon after birth. Interestingly, we also found *Mogat2* expression in the yolk sac, which plays an important role in supplying nutrients for early embryos (28), analogous to the intestine in postnatal life. However, the null mutation of *Mogat2* in the germ line did not lead to apparent intrauterine growth defects, as *Mogat2*$^{-/-}$ fetuses appeared normal and had body weights similar to wild-type and heterozygous littermates at E19. The role of MGAT2 during embryogenesis, if any, appears dispensable. In contrast, MGAT2 is required for normal growth in early postnatal life. *Mogat2*$^{-/-}$ pups grew slower than their wild-type littermates when pups relied on fat-rich mouse milk for calories, consistent with its role in enhancing metabolic efficiency upon high-fat feeding (7, 9).

The effects of nutrition during early postnatal development on long-term energy balance have been demonstrated in several mammalian species (16). Thus, limited weight gain during the suckling period and the compensatory growth after weaning seen in *Mogat2*$^{-/-}$ mice could contribute to the obesity-resistance observed later in life. More importantly, from the prospective of designing an

intervention, these observations raised the question whether inactivating MGAT2 in adulthood can have the same protective effects. Our data suggest that lacking MGAT2 during early development could contribute to obesity resistance later in life; nonetheless, inactivating MGAT2 in adulthood is sufficient to reduce metabolic efficiency and protect mice from metabolic disorders induced by high-fat feeding.

The energy balance phenotypes of *Mogat2*^{AKO} mice resembled those of *Mogat2*$^{-/-}$ mice as well as mice with an intestine-specific MGAT2 deficiency (*Mogat2*^{IKO}) (7, 8). When fed chow or the semipurified diet containing 10 kcal% fat, these MGAT2-deficient mice tended to show increased energy expenditure as well as food intake. Compared with their respective controls, the increases were less pronounced in *Mogat2*^{AKO} and *Mogat2*^{IKO} mice than in *Mogat2*$^{-/-}$ mice; however, all maintained energy balance similar to controls, as reflected by similar body weights during short-term diet challenge in the metabolic chambers. The marked increase in energy expenditure protects *Mogat2*$^{-/-}$ mice against weight gain-induced by a high-refined carbohydrate diet as well as by the Agouti mutation without high-fat feeding (9). It remains to be determined if adult-onset MGAT2 deficiency also reduces propensity to gain weight independent of fat content in diet.

When switched to the high-fat diets, *Mogat2*^{AKO} mice, like *Mogat2*^{IKO} and *Mogat2*$^{-/-}$ mice, were able to adjust to the high caloric content and reduced food intake, with a pronounced reduction on the first day [Fig. 4A (8) and data not shown]. These findings suggest that MGAT2 in the intestine likely modulates short-term food intake regulation in the hypothalamus. The reduction in food intake of *Mogat2*^{AKO} mice contributed to the immediate differences in the initial weight gain to the same extent as observed in *Mogat2*^{IKO} and *Mogat2*$^{-/-}$ mice (8). As control mice acclimatized to high-fat feeding and decreased their food intake, the differences in food intake disappeared (Fig. 4A). In the meantime, the increase in energy expenditure of *Mogat2*^{AKO} mice over control littermates became significant and could explain the increasing differences in weight gain over time.

The molecular mechanisms underlying the effects of inactivating MGAT2 in adults on long-term energy balance are not clear. Intestinal MGAT2 is likely a major contributor. Its expression levels determine the rate of MAG uptake and esterification in enterocytes (8, 10). Deficiency of MGAT2 in the intestine leads to changes in temporal and spatial distribution of fat absorption, which may result in blunted postprandial triglyceridemia as seen in both *Mogat2*$^{-/-}$ and *Mogat2*^{IKO} mice (7, 8, 10). The associated changes in neural and hormonal signals may also contribute to the alterations in food intake, partitioning of energy-yielding nutrients, and systemic energy metabolism. Nonetheless, MGAT2 expressed in other tissues, such as the adipose tissues, may further contribute to the energy balance phenotypes, because both mice expressing MGAT2 and those lacking MGAT2 in an intestine-specific manner exhibit an energy balance phenotypes intermediate between wild-type and global knockout mice (8, 10). These possibilities remain to be tested experimentally.

Interestingly, the difference in energy expenditure between *Mogat2*^{AKO} mice and their littermate controls (Fig. 4C) appeared smaller than the difference between *Mogat2*$^{-/-}$ and wild-type littermates (8), which was consistent with the observation that *Mogat2*^{AKO} mice were protected from diet-induced weight gain to a lesser extent than were *Mogat2*$^{-/-}$ mice (Fig. 1E and Fig. 5A). These findings suggest that lacking MGAT2 during early development may have lasting effects later in life, including increases in energy expenditure. The underlying mechanisms might involve the hypothalamic pathways controlling energy balance, as implicated by findings from studies in which mouse pups are raised in varying litter sizes as well as pups nursed by dams fed different fatty acids (15, 29, 30). On the other hand, even though the levels of *Mogat2* mRNA and MGAT activity in tissues from *Mogat2*^{AKO} mice examined were reduced to levels similar to tissues from *Mogat2*$^{-/-}$ mice, we cannot exclude the possibility that some minor population of cells could retain MGAT2 expression and contribute to the decreased phenotypic differences.

Despite an intermediate effect on prevention of diet-induced weight gain, inactivation of *Mogat2* in adulthood in mice had robust effects on preventing hepatic TAG accumulation. The moderate reduction in weight gain was also associated with improved glucose homeostasis, as indicated by lower levels of fasting glucose and insulin as well as enhanced glucose tolerance compared with controls (Fig. 6), similar to that seen in *Mogat2*$^{-/-}$ mice (7, 8). It is unclear if the role of MGAT2 in hepatic lipid metabolism and glucose homeostasis is completely dependent on its effect on systemic energy balance.

Acute inactivation of MGAT2 in mice that had already gained weight on a high-fat diet also diminished their ability to gain more weight and enhanced their glucose tolerance (Fig. 7); their blood glucose peaked at a lower level, and it declined faster than those of controls after being challenged intragastrically with the same dose of glucose. Further, the differences in glucose tolerance were exacerbated over time. In concert with previous findings that *Mogat2*^{IKO} mice have improved glucose homeostasis (8), these findings indicate that acute inactivation of intestinal MGAT2 may enhance glucose homeostasis, similar to immediate metabolic improvements following some of the bariatric procedures (31).

In summary, our findings indicate that MGAT2 enhances metabolic efficiency and promotes positive energy balance during early development in mice. Nonetheless, inactivation of MGAT2 in adulthood is sufficient to decrease the propensity to gain weight and prevent glucose intolerance when challenged with a calorie-dense diet, even in mice that had already accumulated excess body fat. These findings imply the potential efficacy of MGAT2 as an intervention target for combating obesity and related metabolic diseases caused by chronic caloric surplus. However, the reduction in weight gain is diminished as compared with mice born

without the enzyme, suggesting that MGAT2 can modulate nutritional status in early postnatal life and its deficiency during critical periods may program metabolism later in life.

The authors thank Dr. Guy Groblewski for insightful comments.

REFERENCES

1. Coleman, R. A., and D. P. Lee. 2004. Enzymes of triacylglycerol synthesis and their regulation. *Prog. Lipid Res.* **43:** 134–176.
2. Yen, C. L., D. W. Nelson, and M. I. Yen. Intestinal triacylglycerol synthesis in fat absorption and systemic energy metabolism. *J Lipid Res.* Epub ahead of print. September 17, 2014; doi:10.1194/jlr.R052902.
3. Yen, C. L., S. J. Stone, S. Cases, P. Zhou, and R. V. Farese, Jr. 2002. Identification of a gene encoding MGAT1, a monoacylglycerol acyltransferase. *Proc. Natl. Acad. Sci. USA.* **99:** 8512–8517.
4. Yen, C. L., and R. V. Farese, Jr. 2003. MGAT2, a monoacylglycerol acyltransferase expressed in the small intestine. *J. Biol. Chem.* **278:** 18532–18537.
5. Cao, J., E. Hawkins, J. Brozinick, X. Liu, H. Zhang, P. Burn, and Y. Shi. 2004. A predominant role of acyl-CoA:monoacylglycerol acyltransferase-2 in dietary fat absorption implicated by tissue distribution, subcellular localization, and up-regulation by high fat diet. *J. Biol. Chem.* **279:** 18878–18886.
6. Cheng, D., T. C. Nelson, J. Chen, S. G. Walker, J. Wardwell-Swanson, R. Meegalla, R. Taub, J. T. Billheimer, M. Ramaker, and J. N. Feder. 2003. Identification of acyl coenzyme A:monoacylglycerol acyltransferase 3, an intestinal specific enzyme implicated in dietary fat absorption. *J. Biol. Chem.* **278:** 13611–13614.
7. Yen, C. L., M. L. Cheong, C. Grueter, P. Zhou, J. Moriwaki, J. S. Wong, B. Hubbard, S. Marmor, and R. V. Farese, Jr. 2009. Deficiency of the intestinal enzyme acyl CoA:monoacylglycerol acyltransferase-2 protects mice from metabolic disorders induced by high-fat feeding. *Nat. Med.* **15:** 442–446.
8. Nelson, D. W., Y. Gao, M. I. Yen, and C. L. Yen. 2014. Intestine-specific deletion of acyl-CoA:monoacylglycerol acyltransferase (MGAT) 2 protects mice from diet-induced obesity and glucose intolerance. *J. Biol. Chem.* **289:** 17338–17349.
9. Nelson, D. W., Y. Gao, N. M. Spencer, T. Banh, and C. L. Yen. 2011. Deficiency of MGAT2 increases energy expenditure without high-fat feeding and protects genetically obese mice from excessive weight gain. *J. Lipid Res.* **52:** 1723–1732.
10. Gao, Y., D. W. Nelson, T. Banh, M. I. Yen, and C. L. Yen. 2013. Intestine-specific expression of MOGAT2 partially restores metabolic efficiency in Mogat2-deficient mice. *J. Lipid Res.* **54:** 1644–1652.
11. Kawai, J., A. Shinagawa, K. Shibata, M. Yoshino, M. Itoh, Y. Ishii, T. Arakawa, A. Hara, Y. Fukunishi, H. Konno, et al. 2001. Functional annotation of a full-length mouse cDNA collection. *Nature.* **409:** 685–690.
12. Chon, S. H., Y. X. Zhou, J. L. Dixon, and J. Storch. 2007. Intestinal monoacylglycerol metabolism: developmental and nutritional regulation of monoacylglycerol lipase and monoacylglycerol acyltransferase. *J. Biol. Chem.* **282:** 33346–33357.
13. Hales, C. N., and D. J. Barker. 2001. The thrifty phenotype hypothesis. *Br. Med. Bull.* **60:** 5–20.
14. Duque-Guimarães, D. E., and S. E. Ozanne. 2013. Nutritional programming of insulin resistance: causes and consequences. *Trends Endocrinol. Metab.* **24:** 525–535.
15. Schipper, L., K. Bouyer, A. Oosting, R. B. Simerly, and E. M. van der Beek. 2013. Postnatal dietary fatty acid composition permanently affects the structure of hypothalamic pathways controlling energy balance in mice. *Am. J. Clin. Nutr.* **98:** 1395–1401.
16. Waterland, R. A. 2014. Epigenetic mechanisms affecting regulation of energy balance: many questions, few answers. *Annu. Rev. Nutr.* **34:** 337–355.
17. Levin, B. E. 2000. The obesity epidemic: metabolic imprinting on genetically susceptible neural circuits. *Obes. Res.* **8:** 342–347.
18. McMillen, I. C., and J. S. Robinson. 2005. Developmental origins of the metabolic syndrome: prediction, plasticity, and programming. *Physiol. Rev.* **85:** 571–633.
19. McCance, R. A. 1962. Food, growth, and time. *Lancet.* **2:** 621–626.
20. Ravelli, G. P., Z. A. Stein, and M. W. Susser. 1976. Obesity in young men after famine exposure in utero and early infancy. *N. Engl. J. Med.* **295:** 349–353.
21. Kozak, L. P., S. Newman, P. M. Chao, T. Mendoza, and R. A. Koza. 2010. The early nutritional environment of mice determines the capacity for adipose tissue expansion by modulating genes of caveolae structure. *PLoS ONE.* **5:** e11015.
22. Hayashi, S., and A. P. McMahon. 2002. Efficient recombination in diverse tissues by a tamoxifen-inducible form of Cre: a tool for temporally regulated gene activation/inactivation in the mouse. *Dev. Biol.* **244:** 305–318.
23. Ruzankina, Y., C. Pinzon-Guzman, A. Asare, T. Ong, L. Pontano, G. Cotsarelis, V. P. Zediak, M. Velez, A. Bhandoola, and E. J. Brown. 2007. Deletion of the developmentally essential gene ATR in adult mice leads to age-related phenotypes and stem cell loss. *Cell Stem Cell.* **1:** 113–126.
24. Livak, K. J., and T. D. Schmittgen. 2001. Analysis of relative gene expression data using real-time quantitative PCR and the 2(-Delta Delta C(T)) Method. *Methods.* **25:** 402–408.
25. Teter, B. B., J. Sampugna, and M. Keeney. 1990. Milk fat depression in C57Bl/6J mice consuming partially hydrogenated fat. *J. Nutr.* **120:** 818–824.
26. Barker, N. 2014. Adult intestinal stem cells: critical drivers of epithelial homeostasis and regeneration. *Nat. Rev. Mol. Cell Biol.* **15:** 19–33.
27. Carninci, P., T. Kasukawa, S. Katayama, J. Gough, M. C. Frith, N. Maeda, R. Oyama, T. Ravasi, B. Lenhard, C. Wells, et al. 2005. The transcriptional landscape of the mammalian genome. *Science.* **309:** 1559–1563.
28. Freyer, C., and M. B. Renfree. 2009. The mammalian yolk sac placenta. *J. Exp. Zool. B Mol. Dev. Evol.* **312:** 545–554.
29. Oosting, A., D. Kegler, G. Boehm, H. T. Jansen, B. J. van de Heijning, and E. M. van der Beek. 2010. N-3 long-chain polyunsaturated fatty acids prevent excessive fat deposition in adulthood in a mouse model of postnatal nutritional programming. *Pediatr. Res.* **68:** 494–499.
30. Li, G., J. J. Kohorst, W. Zhang, E. Laritsky, G. Kunde-Ramamoorthy, M. S. Baker, M. L. Fiorotto, and R. A. Waterland. 2013. Early postnatal nutrition determines adult physical activity and energy expenditure in female mice. *Diabetes.* **62:** 2773–2783.
31. Bradley, D., F. Magkos, and S. Klein. 2012. Effects of bariatric surgery on glucose homeostasis and type 2 diabetes. *Gastroenterology.* **143:** 897–912.